

Wearable Data Generation Using Time-Series Generative Adversarial Networks for Hydration Monitoring

Farida Sabry¹^a, Wadha Labda¹^b, Tamer Eltaras¹^c, Fatima Hamza¹^d, Khawla Alzoubi²^e
and Qutaibah Malluhi¹^f

¹*Qatar University, Doha, Qatar*

²*Engineering Technology Department, Community College of Qatar, Doha, Qatar*

Keywords: Data Generation, Synthetic Data, GAN, Wearable Devices, Biosignals.

Abstract: Collection of biosignals data from wearable devices for machine learning tasks can sometimes be expensive and time-consuming and may violate privacy policies and regulations. Successful and accurate generation of these signals can help in many wearable devices applications as well as overcoming the privacy concerns accompanied with healthcare data. Generative adversarial networks (GANs) have been used successfully in generating images in data-limited situations. Using GANs for generating other types of data has been actively researched in the last few years. In this paper, we investigate the possibility of using a time-series GAN (TimeGAN) to generate wearable devices data for a hydration monitoring task to predict the last drinking time of a user. Challenges encountered in the case of biosignals generation and state-of-the-art methods for evaluation of the generated signals are discussed. Results have shown the applicability of using TimeGAN for this task based on quantitative and visual qualitative metrics. Limitations on the quality of the generated signals were highlighted with suggesting ways for improvement.


1 INTRODUCTION


The recent advances in wearable technology have motivated researchers and industry to investigate many machine learning based applications that can learn from the vast amount of signals from wearable sensors (Sabry et al., 2022a). There are a variety of non-invasive signals that can be captured from the human body using different sensors to learn about the health condition of the user for a wide variety of machine learning healthcare applications (Sabry et al., 2022a). Some of the problems that arise with these types of applications are the cost and time associated with the data collection phase, the limited size of datasets used for training (Sabry et al., 2022b; Delmastro et al., 2020). Additionally, the collection of biosignals data is erroneous which increases the cost and time even more. Data collection of health data is subjected to


many regulations to ensure the safety of subjects and preserve the privacy of their sensitive data. Though anonymizing this sensitive data by removing identifying features or adding noise and grouping individuals into broader categories is sometimes done to overcome this privacy problem, it is usually not effective with small dataset sizes used in research from wearable devices.


One way to overcome these problems is to generate synthetic training data that follows the same distribution for real world data (Piacentino et al., 2021; Zhou et al., 2019; Yoon et al., 2019). Synthetic data can be used with various objectives such as data understanding, data imputation (Luo et al., 2018), data correction and noise removal (Kiranyaz et al., 2022; Lu et al., 2021; Zargari et al., 2021), data augmentation (Um et al., 2017; Kiyasseh et al., 2020; Lo et al., 2021; Montero et al., 2021), and data privacy (Xin et al., 2020; Nguyen et al., 2020; Piacentino et al., 2021).


A synthetically generated dataset must have the same mathematical and statistical properties as the real-world dataset. For biosignals generation, there are additional constraints on the shape and repeated pattern of some signals which must be preserved in


^a <https://orcid.org/0000-0001-5639-983X>

^b <https://orcid.org/0000-0001-6097-2395>

^c <https://orcid.org/0000-0002-8664-9091>

^d <https://orcid.org/0000-0002-3689-7003>

^e <https://orcid.org/0000-0002-2797-2673>

^f <https://orcid.org/0000-0003-2849-0569>

synthetic data. The generated data has to be realistic enough to gain true insights from it when used in different machine learning tasks (Sabry et al., 2022a). Synthetic data is less subjected to data privacy concerns or missing values problems. Synthetic data generation has been approached using many techniques that either change the real data to guarantee its privacy such as differential privacy (Ping et al., 2017; Xin et al., 2020; Um et al., 2017) or learn from the real data using a variety of machine-learning techniques (Reiter, 2005; Zhang et al., 2017; Xu et al., 2019; Yoon et al., 2019) to learn the distribution of the data and then sample the distribution to generate the synthetic data.

Generative adversarial networks (GANs) are among the machine learning techniques that can be used to generate synthetic data that is similar to the actual data in terms of data distribution and statistical features. The authors in (Goodfellow et al., 2014) were the first to introduce GAN to generate new synthetic image data that are difficult to be distinguished from real data images but at the same time not memorized from the training set. With the potential of GAN and development of research for its variants, GAN has been used to generate various other types of data such as tabular data with discrete and continuous values (Xu et al., 2019). Although there are some similarities in the used techniques, there are differences in implementation for every type of data which requires some adjustments in the GAN architecture. In this study, we investigate the use of a variant of GAN, specific for time-series data (Yoon et al., 2019), to generate synthetic data of different biosignals which have special characteristics such as amplitude thresholds, repetitive pattern, positions of peaks and troughs to be used for hydration monitoring based on the real dataset we collected in (Sabry et al., 2022b). Though there are some studies (Furdui et al., 2021; Belo et al., 2017; Zhou et al., 2019) that used other types of GANs to generate electrocardiogram (ECG) or galvanic skin response (GSR) signals for other classification tasks, but few studied using GANs for a regression problem (Ning et al., 2018) and for the best of our knowledge this is the first study to use GAN for hydration monitoring data generation to predict the last drinking time.

The rest of the paper is organized as follows. Section 2 reviews briefly the background for this research giving a summarized overview for GAN and its variants. Related work for using GANs for biosignals generation and challenges for biosignals data are discussed in this section as well. Section 3 briefly describes the dataset (Sabry et al., 2022b) used in this research. In section 4, the methodology for us-

ing times-series GAN for synthetic data generation for hydration monitoring is presented, together with the used evaluation metrics. Results and discussion are presented in section 5. The paper is then concluded in section 6 with a summary of the research, its results, its limitations and future improvements are highlighted.

2 BACKGROUND AND RELATED WORK

Generative adversary network (GAN) is a machine learning model that is simply based on two deep neural networks; one is called the generator network (G) and the other is called discriminator network (D) and both of them compete in a zero-sum game to reach Nash equilibrium with a value function $V(D, G)$ given in Equation 1 where x represents the input real samples to the discriminator and z represents the input noise samples to the generator from which it starts to generate fake data $G(z)$. While G works on generating realistic data by minimizing V , D is a classifier that is used to differentiate the real and fake data as genuinely as possible by maximizing V . A typical GAN model is shown in Figure 1, both the generator and discriminator typically have multiple convolution layers to capture the details of the input data. GAN was first introduced by Goodfellow et al (Goodfellow et al., 2014) in 2014 and since then research has been developing different GAN variants that were able to generate images, videos, music notes, etc with high quality. The authors in (Jabbar et al., 2022) review the different variants of GANs, their wide range of applications, shortcomings affecting the training stability and different training solutions.

$$\min_G \max_D V(D, G) = \mathbb{E}_{x \sim p_{data}(x)} [\log D(x)] + \mathbb{E}_{z \sim p_z(z)} [\log (1 - D(G(z)))] \quad (1)$$

The basics for generative modeling in GAN can be seen as improvements to autoencoders. Autoencoder and its probabilistic version, variational autoencoder, are used to represent high-dimensionality data and compress it into a small representation with simple neural networks (encoder and decoder) without massive data loss (Jabbar et al., 2022). Generative models were then used to improve the quality of the generated data and guarantee better privacy protection measures. Here we list some examples for GAN variants used in literature for generation of different biosignals which have special characteristics and challenges dif-

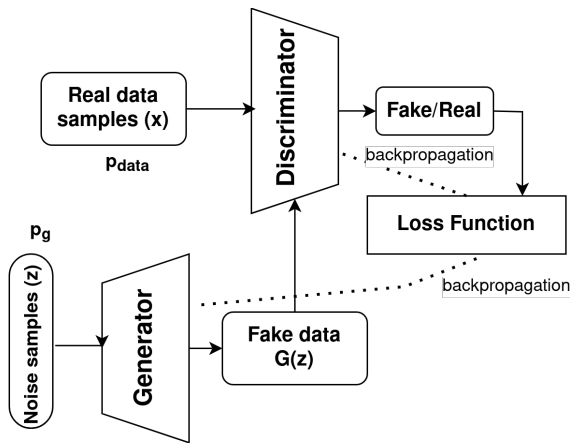


Figure 1: General GAN architecture.

ferent from images that will be discussed in the next subsection.

- **Conditional GAN:** It is very similar to the simple GAN in Figure 1 but with the output of the generator and discriminator conditioning on labels y or any additional information in general for both the real samples and the noise samples as shown in Figure 2 with modified objective function in Equation 2 to improve the diversity of the generated dataset. The first term in the objective function is the expected log likelihood of the real data samples under the discriminator, given the label or context y that the discriminator is trying to predict. The second term is the expected log likelihood of the synthetic data samples under the discriminator, given the label or context y . It has been used in (Kiyasseh et al., 2020) for the generation of pathological photoplethysmogram (PPG) signals in order to boost medical classification performance for different cardiac classes. PPG signals were downsampled and split into overlapping 5sec-frames and fed to three different CGANs which may not handle the temporal behavior of the data and produce unrealistic data. They modified the loss functions with different terms to improve inter-class diversity and penalize the network for generating unrealistic samples. In (Harada et al., 2018), they proposed forming each neural network in GAN based on a recurrent neural network (RNN) using long short-term memories (LSTM) for its hidden layers to deal with the time-series data generation for ECG and EEG signals. An ICU dataset recording oxygen saturation, heart rate, respiratory rate and mean arterial pressure has been used in (Esteban et al., 2017) to generate synthetic data for various ICU prediction tasks of whether a patient

will go in a critical condition defined by thresholds for these variables. They showed that the prediction accuracy decreases when training with synthetic data by a maximum of 12%. Generating synthetic signals for four kinds of biomedical signals (electrocardiogram (ECG), electroencephalogram (EEG), electromyography (EMG), photoplethysmography (PPG)) was done in (Hazra and Byun, 2020). They used a CGAN with bidirectional grid long short-term memory for the generator network and convolutional neural network for the discriminator network to capture time-series dependency.

$$\begin{aligned}
 \min_G \max_D V(D, G) = & \mathbb{E}_{x \sim P_{data}(x)} [\log D(x|y)] + \\
 & \mathbb{E}_{z \sim p_z(z)} [\log (1 - D(G(z|y)))]
 \end{aligned}
 \tag{2}$$

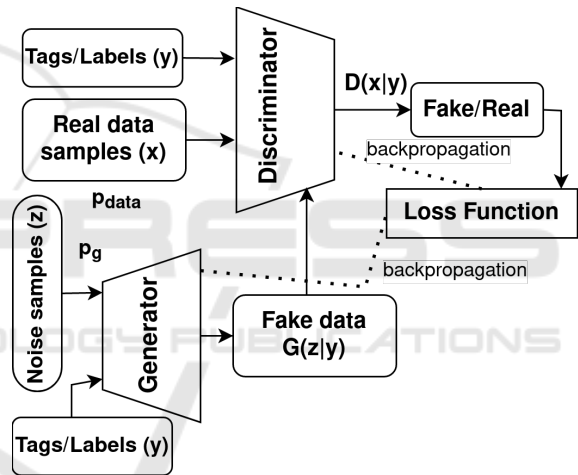


Figure 2: Conditional GAN architecture.

- **Cycle GAN (Zhu et al., 2017):** It is a special kind of conditional GAN where the condition is not a label or tag but rather a sample data from a different domain, in the case of data generation it can be mapping of a sample from synthetic data to real data or vice versa, one GAN works in the forward cycle and the other in the backward, or it can be to transform one raw signal to a derived signal. General architecture for a cycle GAN can be modeled as shown in Figure 3 and its full objective function is given in Equation 3 where adversarial losses for the forward and backward GANs are calculated as in Equation 1 and \mathcal{L}_{cyc} is calculated according to Equation 4 to ensure cycle consistency by reducing the possibilities for the mapping function so that an individual input x_i can be mapped to a desired output y_i . However, cycle GANs require a relatively big dataset

to reduce the replication percentage of the generated data. For biosignals generation, Cycle GAN has been used in (Aqajari et al., 2021) for respiratory rate estimation through learning a mapping of PPG signals to respiratory signals and updating the objective function to include a weighted term that takes into account the respiratory rate of the generated respiratory signals. It has been used in (Zargari et al., 2021) too, for noise artifacts removal without depending on accelerometer data through PPG signal to image transformation. The authors in (Kiranyaz et al., 2022) also used operational cycle-GANs for ECG signals restoration, not whole signal generation. They used quantitative evaluation by measuring the performance gain for peak detection as well as the visual qualitative evaluation.

$$\mathcal{L}(G, F, D_X, D_Y) = \mathcal{L}_{GAN}(G, D_Y, X, Y) + \mathcal{L}_{GAN}(F, D_X, Y, X) + \lambda \mathcal{L}_{cyc}(G, F) \quad (3)$$

$$\mathcal{L}_{cyc}(G, F) = \mathbb{E}_{x \sim P_{data}(x)} [\|F(G(x)) - x\|_1] + \mathbb{E}_{y \sim P_{data}(y)} [\|G(F(y)) - y\|_1] \quad (4)$$

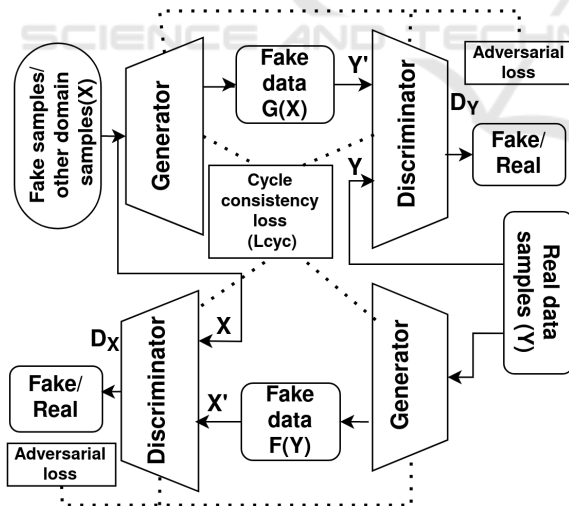


Figure 3: Cycle GAN architecture.

- Wasserstein GAN (W-GAN) (Arjovsky et al., 2017): It is very similar to the traditional GAN but with calculating the loss function based on Wasserstein distance between the real data distribution and the generated data distribution rather than depending on Jensen–Shannon divergence. This GAN variant was introduced to solve mode

collapse problem which is a GAN training challenge. In the context of biosignal generation, an auxiliary conditioned WGAN has been used in (Furdui et al., 2021) to generate galvanic skin response (GSR) and electrocardiogram (ECG) signals that can be used for arousal classification by combining the Wasserstein loss with the gradient penalty and classification loss to discard signals that doesn't improve the classification to enhance the generalizability of emotion recognition algorithms. WGAN was also used with modified Gate Recurrent Units (GRUs) in (Luo et al., 2018) for imputation of data in physionet dataset, authors were able to model the temporal irregularity of the incomplete time series. Their results outperformed the baselines in terms of accuracy of imputation for the missing data during recording process.

- Style Generator Architecture for GAN (Style GAN): It is a modified architecture to GAN where more complexity is added to the generator to have 26.2M trainable parameters (Karras et al., 2021). This is done through adding a mapping network of fully connected layers to map the input to a latent representation, followed by a synthesis network which is controlled by this representation through adaptive instance normalization (AdaIN) at each convolution layer. This aims to achieve better interpolation and also model the factors of variation better, its usage has vastly improved the generation of images that feel-like real. A variant of style GAN was used in (Montero et al., 2021) for fetal brain ultrasound plane classification. It was used in (Thambawita et al., 2021) for generation of gastroenterology data images. To the best of our knowledge, styleGAN hasn't been applied to biosignals with time-series patterns.
- Time-series GAN (Yoon et al., 2019) is another type of GAN that combines the traditional unsupervised GAN network with a supervised autoregressive model to model the temporal dynamics of a time-series. A typical architecture of the TimeGAN is shown in Figure 4. Weights are updated based on three losses; the supervised loss, the unsupervised loss and the reconstruction loss of the autoregressive model defined as in Equations 5, 6 and 7 respectively where the expected log likelihood is calculated over all time steps for both real and synthetic data. It has been used to generate stock and energy prediction data and reported improvement over other CGANs with units that capture temporal dynamics such as RNN and LSTM (Brophy et al., 2021). It hasn't been applied before for biosignals data generation as we

propose in this paper.

$$\mathcal{L}_{supervised} = \mathbb{E}_{s, x_{1:T} \sim p} \left[\sum_t \|h_t - G_X(h_s, h_{t-1}, z_t)\|_2 \right] \quad (5)$$

$$\begin{aligned} \mathcal{L}_{unsupervised} = & \mathbb{E}_{s, x_{1:T} \sim p} [\log(y_s) + \sum_t \log(y_t)] + \\ & \mathbb{E}_{s, x_{1:T} \sim p'} [\log(1 - y'_s) + \sum_t \log(1 - y'_t)] \end{aligned} \quad (6)$$

$$\mathcal{L}_{reconstruction} = \mathbb{E}_{s, x_{1:T} \sim p} [\|s - s'\|_2 + \sum_t \|x_t - x'_t\|_2] \quad (7)$$

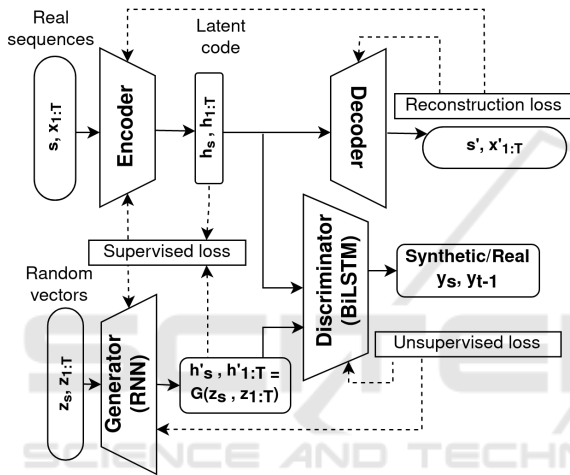


Figure 4: Time-series GAN architecture.

2.1 Challenges of Biosignals Generation

Biosignals dataset collection is considered very challenging for many reasons. Most of the time, the real dataset is with a limited number of subjects due to the cost involved and the privacy constraints. The collected data may suffer from missing/incorrect data due to errors in sensors' attachment or noisy signals due to motion artifacts (Elgendi, 2016). There are other inadequacies that might appear in the collected data which include insufficient measurement time, different sensors' configurations used by different subjects and inconsistent measurement times (Hernangómez et al., 2022). Generative modeling to generate synthetic data based on the real biosignals dataset collected consequently becomes challenging. In addition to the paucity of the collected data and its aforementioned inadequacies, class imbalance data (Kiyasseh et al., 2020) for infected or abnormal samples pose other difficulties for synthetic data generation.

Real-world tabular data collected for biosignals usually consists of mixed types; continuous data for signals from sensors such as photoplethysmography (PPG), ECG, GSR, accelerometer, magnetometer, gyroscope and discrete data such as sex, age, medicine intake, etc. To generate a mix of these discrete and continuous data simultaneously, GANs must apply both softmax and tanh on the output (Xu et al., 2019). Modeling this kind of mixed tabular data in general to generate realistic data is a non-trivial task (Xu et al., 2019). A review for some approaches to handle discrete data is presented in (Jabbar et al., 2022). Continuous data for biosignals usually follow a non-Gaussian distribution unlike the images pixel values which follow a Gaussian-like distribution. In GANs, the last layer has a tanh function which can successfully output a value in the range $[-1, 1]$ for images data after normalization using a min-max transformation whereas continuous non-Gaussian data will lead to vanishing gradient problem.

As well known in the machine learning field, highly imbalanced data poses many challenges for learning in general and for learning a GAN model in particular as minority classes are underrepresented making a GAN susceptible to severe mode collapse. In this case, the generator produce outputs with small diversity leading to only slight changes to the data distribution that may be hardly detected by the discriminator. To decrease this effect and prevent the generator from optimizing for a single fixed discriminator, Wasserstein loss is used to avoid the discriminator being stuck in local minima. Unrolled GAN (Metz et al., 2017) is another way to face this problem which uses a generator loss function based on the current and future discriminator's classifications so that the generator don't optimize for a single discriminator.

In the next subsection, we review the state-of-art evaluation metrics to evaluate GANs.

2.2 Evaluation Metrics

Evaluation of GAN models is an active research area regarding unstable training (Jabbar et al., 2022) as there is no standard function for evaluation. In this section, we briefly review the different evaluation metrics used in literature to evaluate the GAN and outputs generated by it.

Evaluation metrics can be classified as qualitative or quantitative. Qualitative evaluation refers to human visual assessment for the generated samples from the GAN but it lacks a suitable objective evaluation metric. Quantitative evaluation refers to objective metrics that either assess the similarity of the generated synthetic data to the real data, calculate the distance be-

tween the two distributions or evaluate the accuracy for the classification task or regression error when replacing the real dataset with synthetic dataset for training the machine learning model. Most of the proposed metrics in literature are applicable to the image data (Brophy et al., 2021).

For image data, inception-score (IS) and Fréchet inception distance (FID) are most commonly used to evaluate the diversity and quality of the generated samples for its correlation with human findings of the generated samples (Jabbar et al., 2022).

Pearson correlation coefficient was used in (Hazra and Byun, 2020) to verify the quality of synthetic data when compared to the original data as well as root mean square error (RMSE), percent root mean square difference (PRD), mean absolute error (MAE), and Fréchet distance (FD) for statistical analysis. However, they were used as one-to-one measure between synthetic data and original data used to generate it with assumption of having the same sequence length as the original data (aligned sequences of fixed length).

Propensity score which represents the probabilities of whether a record is real or synthetic, has been used for many record data (Dankar and Ibrahim, 2021). It involves building a binary classification model for classification but not formulated for time-series data. To deal with time-series data, authors in (Yoon et al., 2019) introduced a discriminative score as a quantitative measure for similarity using a 2-layer LSTM to classify sequences as either synthetic or original. The classification error is the score and the less error means the generated sequences are similar to the original data. They also introduced a predictive score which is similar to the Train on Synthetic, Test on Real where a sequence-prediction model with 2-layer LSTM is trained to predict next-step temporal vectors over each input sequence. Then, the trained model is tested on the original dataset. For visualizing how closely the distribution of generated data represents that of the original, authors in (Yoon et al., 2019) used t-Stochastic Neighbor Embedding (t-SNE) (van der Maaten and Hinton, 2008) and principal component analysis (PCA) (Bryant and Yarnold, 2001) by flattening the temporal dimension on both the original and synthetic datasets and results are assessed visually.

As can be deduced from the above brief review, there are no standard evaluation metric for fair model-to-model comparison and specially when it comes to time-series data. The development of a quantitative evaluation metric for the synthetic data generation still requires future research, especially for time-series data. As this is not the main focus of the pa-

per, we chose to use the scores used by (Yoon et al., 2019) as they are the only ones developed for time sequences. Additionally, we used Train on Synthetic Test on Real (TSTR) metric as this is the main goal for the generation of synthetic data to use more data for learning a model that can predict the output value in the regression problem of hydration monitoring for the last drinking time.

3 DATASET

For generating wearable device data for the task of hydration monitoring, we used the real dataset we collected in (Sabry et al., 2022b) using sensors from the calibrated Shimmer Galvanic Skin Response (GSR) unit¹. The last time for water and food intake was recorded for subjects wearing the GSR unit who fasted during Ramadan or were voluntary fasting with no restrictions on movement or the time of wearing the device and also in non-fasting conditions, i.e. the last drinking time is within 1 hour. The signals are recorded from the shimmer device at a frequency of 512 Hz and include PPG, GSR Skin Resistance, GSR Skin Conductance, accelerometer in the three directions (X,Y,Z), magnetometer (X,Y,Z), gyroscope (X,Y,Z), ambient temperature and pressure. A total of 3386 min (56.4 h) data were collected from 11 healthy subjects (9 females and 2 males). All data collection was subject to Qatar University Institutional Review Board (IRB) approval procedures covered by the IRB approval: QU-IRB 1538-EA/21. The raw dataset is available at Zenodo².

4 WEARABLE DATA GENERATION

The approach followed for generating wearable data that can be used for hydration monitoring task in (Sabry et al., 2022b) can be presented as shown in Figure 5. First, a real dataset was built of the biosignals from the wearable device (PPG, GSR) as well as that of the movement sensors (accelerometer, magnetometer and gyroscope) and the ambient temperature and pressure sensors as discussed in the previous section. Preprocessing of the dataset included down-sampling the signals at 1 min intervals and extracting features from signals aggregating the mean val-

¹<http://www.shimmersensing.com/products/gsr-optical-pulse-development-kit> (accessed on 16 Nov. 2022)

²<https://zenodo.org/record/6299964> (accessed on 16 Nov. 2022)

ues and calculating the accumulated changes in the magnitude for accelerometer, magnetometer and gyroscope data (Sabry et al., 2022b) as in Equations 8, 9, 10, 11, 12 and 13. $|ACC|$ refers to the magnitude of the accelerometer from the components in the three directions ($acc_{x_t}, acc_{y_t}, acc_{z_t}$). $cumAcc$ is the accumulative change in accelerometer magnitude over time. $|MAG|$ refers to the magnitude of the magnetometer from the components in the three directions ($mag_{x_t}, mag_{y_t}, mag_{z_t}$). $cumMag$ is the accumulative change in magnetometer magnitude over time. $|GYRO|$ refers to the magnitude of the gyroscope from the components in the three directions ($gyro_{x_t}, gyro_{y_t}, gyro_{z_t}$). $cumGyro$ is the accumulative change in gyroscope magnitude over time. These magnitude values for accelerometer, magnetometer and gyroscope as well as the accumulative changes in them that represent the motion jerk can reflect the effort and state of activity of the subject. For the hydration monitoring task, the fine details of the signals is not as relevant as the big changes of it through time so downsampling and aggregation can be seen feasible. It also helps in speeding up the training of the generative adversary network for time-series data (TimeGAN).

The output signals together with the column for the recorded last drinking time for each of the fasting and non-fasting samples for each subject are then input to the TimeGAN module and are considered the real sequences. The TimeGAN generator uses gated recurrent units in its recurrent neural network with 20 hidden nodes in each of its three layers and the discriminator uses bidirectional long short-term memory units to increase the amount of information available to the network. The generated synthetic signals are then updated with the objective to minimize the three loss functions in Equations 5, 6 and 7 for 500 iterations. The TimeGAN is then evaluated using discriminative score (Yoon et al., 2019) mentioned in section 2.2 with lower value means better. It represents the post-hoc classification error for a supervised classifier fed with original signals labeled as real examples and generated signals labeled as synthetic examples and tested with a held-out test set. A predictive score is also calculated to evaluate the effectiveness of TimeGAN to capture the conditional distributions over time. It represents the mean absolute error (MAE) in predicting the next-step temporal vectors over each input sequence in the original dataset using an LSTM model trained with the synthetic generated dataset.

Training on synthetic data and testing on real was done for the main problem of hydration monitoring where we trained the three models that achieved the

Table 1: Mean discriminative and predictive scores for generated fasting and non-fasting data.

	Discriminative score	Predictive score
fasting	0.319	3.9
non-fasting	0.225	0.276

best performance in (Sabry et al., 2022b); random forest, gradient boosted regression and extra trees.

$$|ACC| = \sqrt{(acc_{x_t}^2 + acc_{y_t}^2 + acc_{z_t}^2)} \quad (8)$$

$$cumAcc = \sum_{j=1}^{t-1} |ACC|_{j+1} - |ACC|_j \quad (9)$$

$$|MAG| = \sqrt{(mag_{x_t}^2 + mag_{y_t}^2 + mag_{z_t}^2)} \quad (10)$$

$$cumMag = \sum_{j=1}^{t-1} |MAG|_{j+1} - |MAG|_j \quad (11)$$

$$|GYRO| = \sqrt{(gyro_{x_t}^2 + gyro_{y_t}^2 + gyro_{z_t}^2)} \quad (12)$$

$$cumGyro = \sum_{j=1}^{t-1} |GYRO|_{j+1} - |GYRO|_j \quad (13)$$

5 RESULTS

5.1 Quantitative Evaluation

The synthetic output of the TimeGAN is evaluated quantitatively using the discriminative and predictive scores for the output of TimeGAN obtained after training for 500 iterations as shown in Table 1. The results show that the average predictive score for generating fasting samples is relatively high, this can be attributed to the smaller number of samples and shorter sequences used in training the TimeGAN with fasting sequences as well as the missing of some other features in the original dataset we used in (Sabry et al., 2022b) such as height, weight, sex and age which affect these signals differently during fasting.

The generation with different fasting and nonfasting samples in the dataset from different subjects was used to check for the relation between the discriminative and predictive scores and the length of the generated sequences. The results are shown in Figure 6 and no relation can be inferred for the dependence of these scores on the length of the generated sequence.

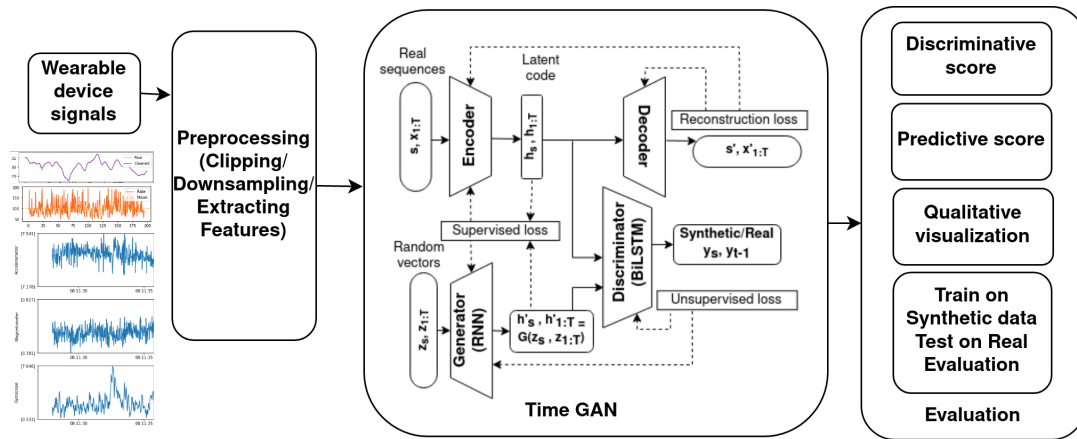


Figure 5: Overview of the wearable data generation steps.

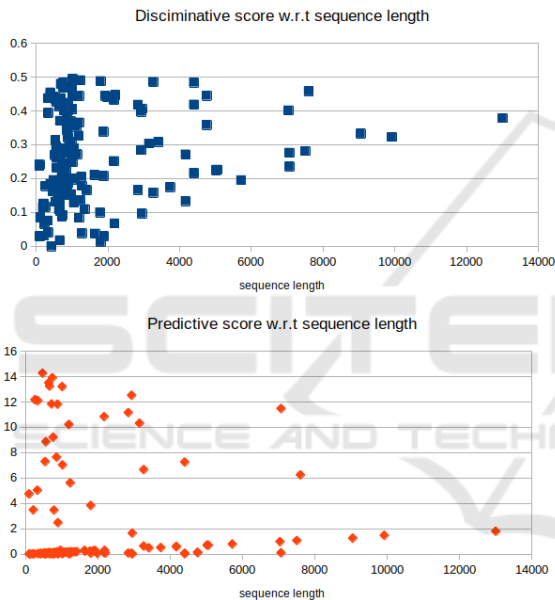


Figure 6: Discriminative score (a) and predictive score (b) vs generated sequence length.

5.2 Qualitative Visualization

As for the qualitative visualization to assess how the distribution of the generated signals is close to that of the real signal, flattening of the time-series sequence for all signals was done using the functions provided by the authors of (Yoon et al., 2019). PCA and t-SNE visualizations are shown in Figure 8 for both fasting and non-fasting sequences. The figure shows the synthetic data projections are closely following that of the original data for these groups of sequences and the rest of sequences show similar closeness with few exceptions. A collective quantitative metric is preferably to be introduced to evaluate the overall distance from the original distribution for all sequences.

Plotting samples of the generated signals separately however doesn't show good quality signals most of the time e.g. an electrodermal activity signal in Figure 7 plotted from a GSR generated signal.

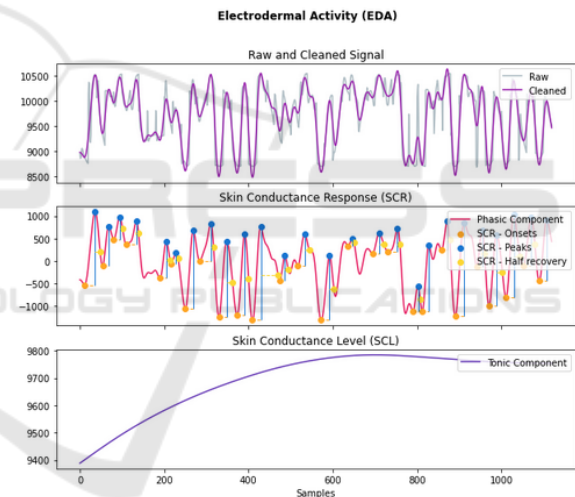


Figure 7: Galvanic skin response generated sample.

5.3 Training on Synthetic Test on Real

The results of the hydration monitoring task for predicting the last drinking time were evaluated by generating balanced synthetic data for fasting and non-fasting since the original data was having more non-fasting samples. Different synthetic data sizes were generated and used for training the best performing models in (Sabry et al., 2022b), namely random forest, gradient boosted regression and extra trees. The average results for 10 runs are shown in Figure 9. It can be shown in the three graphs in Figure 9 that using synthetic data has decreased the root-mean-square error for prediction with respect to training with the small unbalanced real dataset (TRTR) represented by

the red line on top of the graphs with a best case of approximately 1 hour difference in the case of using Gradient Boosted Regressor to predict the last drinking time. The best RMSEs are achieved especially for cases when the real dataset sizes used for training are less than 1500 samples, after that the differences in the accuracy in prediction between using generated data and real data in training start to shrink. This suggests the feasibility of generation of wearable data biosignals using TimeGAN to predict the last drinking time in a hydration monitoring application especially in cases of small real dataset sizes collected. As pointed out in (Sabry et al., 2022b), predicting the last drinking time can provide the flexibility of adjusting the alerting threshold on the wearable device based on the health conditions, needs, and activity of the user. The alerted user/caregiver can then choose to input the correct drinking time if the prediction was not accurate for his/her situation to enable a closed-loop solution with online training to take place to improve the model’s accuracy.

6 CONCLUSION

In this paper, we proposed using a generative adversarial networks model, specifically designed for time-series data, known as TimeGAN (Yoon et al., 2019) to test its applicability for generating wearable biosignals data. It was able to generate the synthetic wearable data signals with low discriminative and predictive scores. Low discriminative score means a classifier can’t distinguish between original and synthetic dataset samples. Low predictive score means that the post-hoc sequence-prediction model is able to predict next-step temporal data signals for each input sequence. Visual evaluation also showed that most of the generated signals are following the same distribution of the original data. Training with synthetic data and testing on real (TSTR) also showed that using synthetic data has decreased the root mean square error (RMSE) for the regression task of predicting the last drinking time compared to the training on real testing on real (TRTR) for using different synthetic data sizes.

One of the main objectives of biosignal wearable data generation is to protect the privacy of the users’ data used in training, another evaluation metric needs to be added to assess TimeGAN’s privacy and its resistance to leak real data that participated in the training by just the GAN memorising it (Bounliphone et al., 2016; Esteban et al., 2017). Another metric for every type of synthetic biosignal generated could be evaluated to test the quality of the generated

signals and possibly categorize them like classifying PPG signals quality in (Elgendi, 2016).

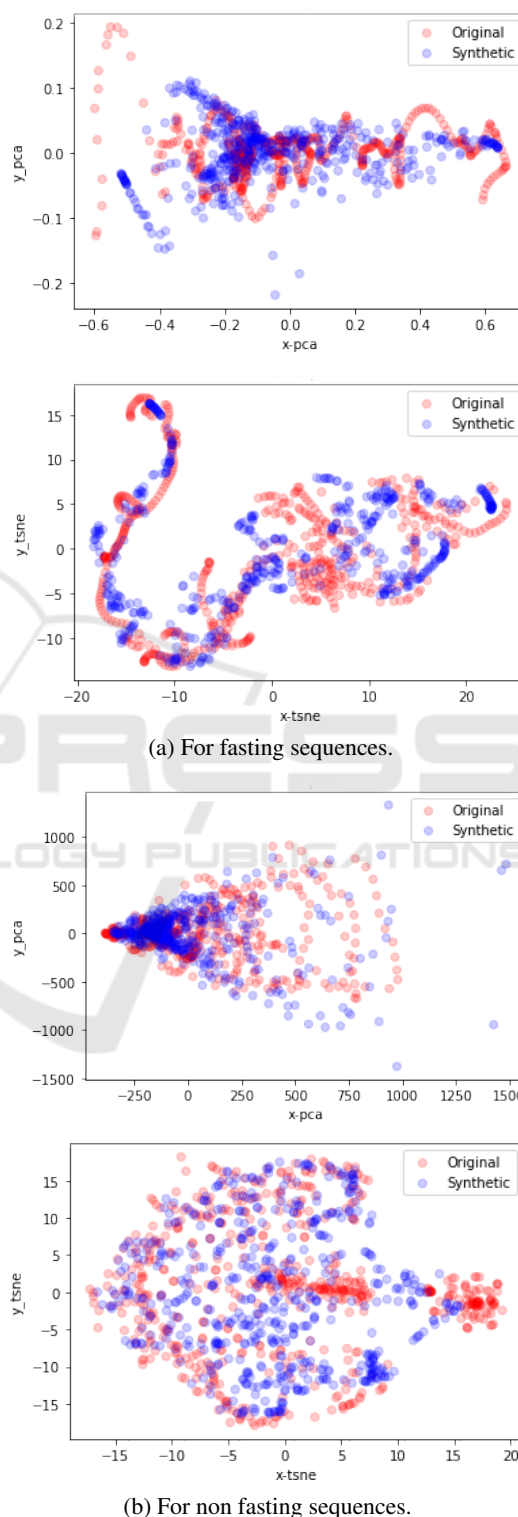
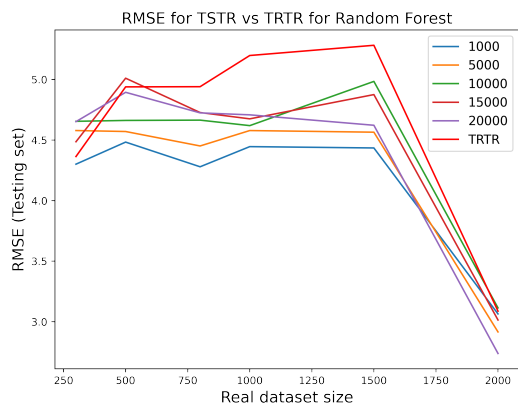
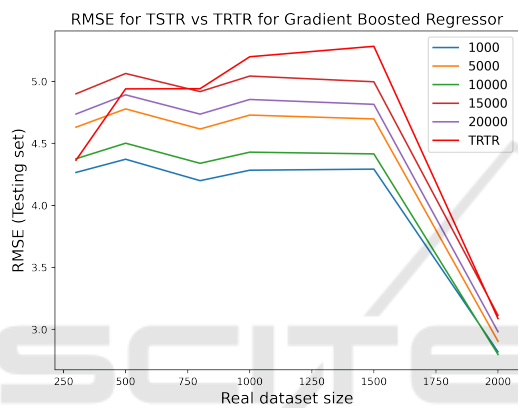


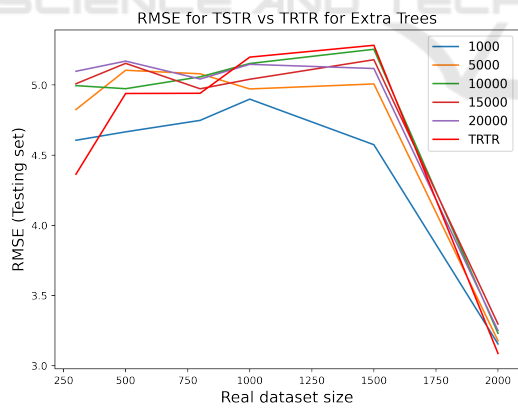
Figure 8: Qualitative PCA and tSNE visualization for fasting and non-fasting sequences.



(a) Random Forest.



(b) Gradient Boosted Regressor.



(c) Extra trees.

Figure 9: Train Synthetic Test Real vs Train Real Test Real for different models.

ACKNOWLEDGEMENTS

This publication was made possible by a grant from the Qatar National Research Fund (QNRF), Project Number ECRA 01-006-1-001. The contents of this

research are solely the responsibility of the authors and do not necessarily represent the official views of the Qatar National Research Fund (QNRF).

REFERENCES

- Aqajari, S. A. H., Cao, R., Zargari, A. H. A., and Rahmani, A. M. (2021). An End-to-End and Accurate PPG-based Respiratory Rate Estimation Approach Using Cycle Generative Adversarial Networks. *arXiv:2105.00594 [cs, eess]*. arXiv: 2105.00594.
- Arjovsky, M., Chintala, S., and Bottou, L. (2017). Wasserstein gan.
- Belo, D., Rodrigues, J., and Vaz, J. (2017). Biosignals learning and synthesis using deep neural networks. *BioMed Eng Online*, 16.
- Bounliphone, W., Belilovsky, E., Blaschko, M. B., Antonoglou, I., and Gretton, A. (2016). A test of relative similarity for model selection in generative models. In Bengio, Y. and LeCun, Y., editors, *4th International Conference on Learning Representations, ICLR 2016, San Juan, Puerto Rico, May 2-4, 2016, Conference Track Proceedings*.
- Brophy, E., Wang, Z., She, Q., and Ward, T. (2021). Generative adversarial networks in time series: A survey and taxonomy. *arXiv*.
- Bryant, F. and Yarnold, P. (2001). *Principal-component analysis and exploratory and confirmatory factor analysis*. American Psychological Association.
- Dankar, F. K. and Ibrahim, M. (2021). Fake it till you make it: Guidelines for effective synthetic data generation. *Applied Sciences*, 11(5).
- Delmastro, F., Martino, F. D., and Dolciotti, C. (2020). Cognitive Training and Stress Detection in MCI Frail Older People Through Wearable Sensors and Machine Learning. *IEEE Access*, 8:65573–65590.
- Elgendi, M. (2016). Optimal signal quality index for photoplethysmogram signals. *Bioengineering (Basel, Switzerland)*, 3(21).
- Esteban, C., Hyland, S. L., and Rätsch, G. (2017). Real-valued (Medical) Time Series Generation with Recurrent Conditional GANs.
- Furdui, A., Zhang, T., Worring, M., Cesar, P., and El Ali, A. (2021). Ac-wgan-gp: Augmenting ecg and gsr signals using conditional generative models for arousal classification. In *Adjunct Proceedings of the 2021 ACM International Joint Conference on Pervasive and Ubiquitous Computing and Proceedings of the 2021 ACM International Symposium on Wearable Computers, UbiComp '21*, page 21–22, New York, NY, USA. Association for Computing Machinery.
- Goodfellow, I., Pouget-Abadie, J., Mirza, M., Xu, B., Warde-Farley, D., Ozair, S., Courville, A., and Bengio, Y. (2014). Generative adversarial nets. In Ghahramani, Z., Welling, M., Cortes, C., Lawrence, N., and Weinberger, K., editors, *Advances in Neural Information Processing Systems*, volume 27. Curran Associates, Inc.

- Harada, S., Hayashi, H., and Uchida, S. (2018). Biosignal data augmentation based on generative adversarial networks. volume 2018, pages 368–371.
- Hazra, D. and Byun, Y.-C. (2020). SynSigGAN: Generative Adversarial Networks for Synthetic Biomedical Signal Generation. *Biology*, 9(12):441.
- Hernangómez, R., Visentin, T., Servadei, L., Khodabakhshandeh, H., and Stańczak, S. (2022). Improving Radar Human Activity Classification Using Synthetic Data with Image Transformation. *Sensors*, 22(4):1519.
- Jabbar, A., Li, X., and Omar, B. (2022). A Survey on Generative Adversarial Networks: Variants, Applications, and Training. *ACM Computing Surveys*, 54(8):1–49.
- Karras, T., Laine, S., and Aila, T. (2021). A style-based generator architecture for generative adversarial networks. *IEEE Transactions on Pattern Analysis and Machine Intelligence*, 43(12):4217–4228.
- Kiranyaz, S., Devecioglu, O., Ince, T., Malik, J., Chowdhury, M., Hamid, T., Mazhar, R., Khandakar, A., Tahir, A., Rahman, T., and Gabbouj, M. (2022). Blind ecg restoration by operational cycle-gans. *IEEE Trans Biomed Eng.*
- Kiyasseh, D., Tadesse, G. A., Nhan, L. N. T., Van Tan, L., Thwaites, L., Zhu, T., and Clifton, D. (2020). PlethAugment: GAN-Based PPG Augmentation for Medical Diagnosis in Low-Resource Settings. *IEEE Journal of Biomedical and Health Informatics*, 24(11):3226–3235.
- Lo, J., Cardinell, J., Costanzo, A., and Sussman, D. (2021). Medical Augmentation (Med-Aug) for Optimal Data Augmentation in Medical Deep Learning Networks. *Sensors*, 21(21):7018.
- Lu, H., Han, H., and Zhou, S. K. (2021). Dual-GAN: Joint BVP and Noise Modeling for Remote Physiological Measurement. In *2021 IEEE/CVF Conference on Computer Vision and Pattern Recognition (CVPR)*, pages 12399–12408, Nashville, TN, USA. IEEE.
- Luo, Y., Cai, X., Zhang, Y., and Xu, J. (2018). Multivariate Time Series Imputation with Generative Adversarial Networks. page 12.
- Metz, L., Poole, B., Pfau, D., and Sohl-Dickstein, J. (2017). Unrolled generative adversarial networks. In *International Conference on Learning Representations*.
- Montero, A., Bonet-Carne, E., and Burgos-Artizzu, X. P. (2021). Generative Adversarial Networks to Improve Fetal Brain Fine-Grained Plane Classification. *Sensors*, 21(23):7975.
- Nguyen, H., Zhuang, D., Wu, P.-Y., and Chang, M. (2020). AutoGAN-based dimension reduction for privacy preservation. *Neurocomputing*, 384:94–103.
- Ning, X., Yao, L., Wang, X., Benatallah, B., Zhang, S., and Zhang, X. (2018). Data-Augmented Regression with Generative Convolutional Network. In Hacid, H., Cellary, W., Wang, H., Paik, H.-Y., and Zhou, R., editors, *Web Information Systems Engineering – WISE 2018*, volume 11234, pages 301–311. Springer International Publishing, Cham. Series Title: Lecture Notes in Computer Science.
- Piacentino, E., Guarner, A., and Angulo, C. (2021). Generating synthetic ecgs using gans for anonymizing healthcare data. *Electronics*, 10(4):389.
- Ping, H., Stoyanovich, J., and Howe, B. (2017). Data-synthesizer: Privacy-preserving synthetic datasets. In *Proceedings of the 29th International Conference on Scientific and Statistical Database Management, SS-DBM '17*, New York, NY, USA. Association for Computing Machinery.
- Reiter, J. P. (2005). Using cart to generate partially synthetic public use microdata. *Journal of Official Statistics*, 21:441–462.
- Sabry, F., Eltaras, T., Labda, W., Alzoubi, K., and Malluhi, Q. (2022a). Machine learning for healthcare wearable devices: The big picture. *Journal of Healthcare Engineering*.
- Sabry, F., Eltaras, T., Labda, W., Hamza, F., Alzoubi, K., and Malluhi, Q. (2022b). Towards on-device dehydration monitoring using machine learning from wearable device’s data. *Sensors*, 22(5).
- Thambawita, V., Hicks, S., Isaksen, J., Stensen, M., Haugen, T., Kanters, J., Parasa, S., de Lange, T., Johansen, H., Johansen, D., Hammer, H., Halvorsen, P., and Riegler, M. (2021). Deepsynthbody: the beginning of the end for data deficiency in medicine. pages 1–8.
- Um, T. T., Pfister, F. M. J., Pichler, D., Endo, S., Lang, M., Hirche, S., Fietzek, U., and Kulić, D. (2017). Data Augmentation of Wearable Sensor Data for Parkinson’s Disease Monitoring using Convolutional Neural Networks. In *Proceedings of the 19th ACM International Conference on Multimodal Interaction*, pages 216–220. arXiv:1706.00527 [cs].
- van der Maaten, L. and Hinton, G. (2008). Visualizing data using t-sne. *Journal of Machine Learning Research*, 9(86):2579–2605.
- Xin, B., Yang, W., Geng, Y., Chen, S., Wang, S., and Huang, L. (2020). Private FL-GAN: Differential Privacy Synthetic Data Generation Based on Federated Learning. In *ICASSP 2020 - 2020 IEEE International Conference on Acoustics, Speech and Signal Processing (ICASSP)*, pages 2927–2931, Barcelona, Spain. IEEE.
- Xu, L., Skoularidou, M., Cuesta-Infante, A., and Veeramachaneni, K. (2019). Modeling Tabular data using Conditional GAN. *arXiv*, page 11.
- Yoon, J., Jarrett, D., and Schaar, M. (2019). Time-series generative adversarial networks. In Wallach, H., Larochelle, H., Beygelzimer, A., d’Alché-Buc, F., Fox, E., and Garnett, R., editors, *Advances in Neural Information Processing Systems*, volume 32. Curran Associates, Inc.
- Zargari, A. H. A., Aqajari, S. A. H., Khodabandeh, H., Rahmani, A. M., and Kurdahi, F. (2021). An Accurate Non-accelerometer-based PPG Motion Artifact Removal Technique using CycleGAN. *arXiv:2106.11512 [cs]*. arXiv: 2106.11512.
- Zhang, J., Cormode, G., Procopiuc, C. M., Srivastava, D., and Xiao, X. (2017). Privbayes: Private data release via bayesian networks. *ACM Trans. Database Syst.*, 42(4).

- Zhou, B., Liu, S., Hooi, B., Cheng, X., and Ye, J. (2019). BeatGAN: Anomalous Rhythm Detection using Adversarially Generated Time Series. In *Proceedings of the Twenty-Eighth International Joint Conference on Artificial Intelligence*, pages 4433–4439, Macao, China. International Joint Conferences on Artificial Intelligence Organization.
- Zhu, J.-Y., Park, T., Isola, P., and Efros, A. A. (2017). Unpaired image-to-image translation using cycle-consistent adversarial networks.

